Sensors and Actuators A 154 (2009) 229–237

Contents lists available at ScienceDirect

Sensors and Actuators A: Physical

journal homepage: www.elsevier.com/locate/sna

Micromachined resonators of high Q-factor based on atomic layer deposited alumina

Yuan-Jen Chang[a,*], Jason M. Gray[b], Atif Imtiaz[c], Dragos Seghete[d], T. Mitch Wallis[c], Steven M. George[d], Pavel Kabos[c], Charles T. Rogers[b], Victor M. Bright[a]

[a] Department of Mechanical Engineering, University of Colorado at Boulder, Boulder, CO 80309, USA
[b] Department of Physics, University of Colorado at Boulder, Boulder, CO 80309, USA
[c] National Institute of Standards and Technology, Boulder, CO 80305, USA
[d] Department of Chemistry and Biochemistry, University of Colorado at Boulder, Boulder, CO 80309, USA

ARTICLE INFO

Article history:
Received 1 April 2008
Received in revised form
11 September 2008
Accepted 10 November 2008
Available online 27 November 2008

Keywords:
Atomic layer deposition
Alumina
Micro-resonator
Resonant frequency
SEM
AFM

ABSTRACT

In this paper, atomic layer deposited (ALD) alumina (Al_2O_3) has been demonstrated as the structural material for a micro-resonator for the first time. An electrostatically actuated micro-bridge made of chromium (Cr) coated ALD Al_2O_3 was used as a resonator. The resonator was formed by simple wet- and dry-etching processes. The static displacement profile of the micro-resonator under electrostatic load was measured by an optical interferometer. A model of a pinned–pinned beam with axial stress of 250 MPa was used to fit the measured data. Two techniques based on scanning electron microscope (SEM) and atomic force microscope (AFM) were developed to characterize the resonant frequencies of different modes and quality factor of the resonator. The measured resonant frequencies match well with the calculated values with residual stress of 258 MPa, providing additional insight into resonator model and ALD alumina material properties. The developed techniques can be applied to further size reduction of devices made with ALD methods.

1. Introduction

Micro- and nano-resonators can be used as sensors of pressure, mass, or force with extremely high resolution. Resonators made of silicon [1] and aluminum nitride [2] have been demonstrated by standard processes, such as chemical vapor deposition (CVD). The processes for forming these materials, however, require high temperatures. Atomic layer deposition (ALD) is a thin film technique that can deposit films at low temperatures, some even less than 100 °C. The ALD process forms a dense, smooth film with atomic-level thickness control. These characteristics are appealing for nano-scale mechanical devices. Previously, ALD Al_2O_3 has been used in MEMS as a protective coating [3]. Additionally, nano-scale structures made of ALD Al_2O_3 have been used to measure the mechanical properties of the ALD thin film [4]. An electrostatically actuated nano-membrane made of ALD Al_2O_3 has been demonstrated [5]. With an ALD hydrophobic coating, the ALD Al_2O_3 has been demonstrated as a bio-compatible material [6]. ALD Al_2O_3 with nanometer-scale thickness used as the structural material for a resonator has been fabricated and characterized [7]. In this paper, the electrostatically actuated micro-resonators made of Cr-coated ALD Al_2O_3 are fabricated, as initially described previously [7]. The displacements of the resonators at different applied voltages have been modeled and experimentally verified. Two new techniques, one based on mechanical excitation and the other based on electrical excitation, are then developed to measure the resonant frequency for micro-/nano-scale thin film resonators. From those measurements, the residual stress inside the structure is verified to be 258 MPa. The information of stress can be used for the design of micro-/nano-devices made of ALD alumina coated with Cr metallic layer. Furthermore, the fabrication and characterization techniques developed here are applicable to further size reduction and design of MEMS/NEMS devices based on atomic layer deposited materials. The new techniques for measurement in Sections 5 and 6 provide an excellent platform for the measurement of nano-devices.

2. ALD alumina

ALD is based on an AB binary gas-phase surface reaction sequence as shown in Fig. 1 [8]. The A precursor is introduced into the viscous flow reactor and reacts with all of the hydroxyl surface sites on the substrate. When there are no more surface sites

* Corresponding author. Tel.: +1 303 492 6107; fax: +1 303 492 3498.
E-mail address: changy@colorado.edu (Y.-J. Chang).

0924-4247/$ – see front matter © 2008 Elsevier B.V. All rights reserved.
doi:10.1016/j.sna.2008.11.015

Report Documentation Page

Form Approved
OMB No. 0704-0188

1. REPORT DATE	2. REPORT TYPE	3. DATES COVERED
SEP 2008		**00-00-2008 to 00-00-2008**

4. TITLE AND SUBTITLE	5a. CONTRACT NUMBER
Micromachined resonators of high Q-factor based on atomic layer deposited alumina	5b. GRANT NUMBER
	5c. PROGRAM ELEMENT NUMBER
6. AUTHOR(S)	5d. PROJECT NUMBER
	5e. TASK NUMBER
	5f. WORK UNIT NUMBER
7. PERFORMING ORGANIZATION NAME(S) AND ADDRESS(ES) **University of Colorado,Department of Chemistry and Biochemistry,Boulder,CO,80309**	8. PERFORMING ORGANIZATION REPORT NUMBER
9. SPONSORING/MONITORING AGENCY NAME(S) AND ADDRESS(ES)	10. SPONSOR/MONITOR'S ACRONYM(S)
	11. SPONSOR/MONITOR'S REPORT NUMBER(S)

12. DISTRIBUTION/AVAILABILITY STATEMENT
Approved for public release; distribution unlimited

13. SUPPLEMENTARY NOTES

14. ABSTRACT

In this paper, atomic layer deposited (ALD) alumina (Al2O3) has been demonstrated as the structural material for a micro-resonator for the first time. An electrostatically actuated micro-bridge made of chromium (Cr) coated ALD Al2O3 was used as a resonator. The resonatorwas formed by simplewet- and dry-etching processes. The static displacement profile of the micro-resonator under electrostatic load was measured by an optical interferometer. A model of a pinned?pinned beam with axial stress of 250MPa was used to fit the measured data. Two techniques based on scanning electron microscope (SEM) and atomic force microscope (AFM) were developed to characterize the resonant frequencies of different modes and quality factor of the resonator. The measured resonant frequencies matchwell with the calculated values with residual stress of 258MPa, providing additional insight into resonator model and ALD alumina material properties. The developed techniques can be applied to further size reduction of devices made with ALD methods.

15. SUBJECT TERMS

16. SECURITY CLASSIFICATION OF:			17. LIMITATION OF ABSTRACT	18. NUMBER OF PAGES	19a. NAME OF RESPONSIBLE PERSON
a. REPORT **unclassified**	b. ABSTRACT **unclassified**	c. THIS PAGE **unclassified**	**Same as Report (SAR)**	**9**	

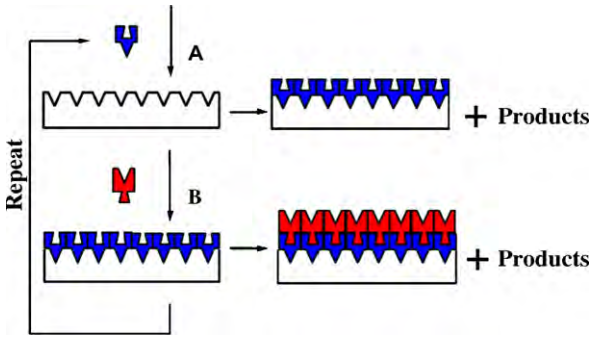

Fig. 1. AB binary surface reaction sequence for ALD.

available, the reactions stop, making this a self-limiting process. The unreacted precursor and the reaction byproducts are then purged from the chamber with nitrogen flow. The B precursor is then introduced into the chamber to react with all of the available methyl sites on the A layer. This is again a self-limiting process, and regenerates the original surface conditions. The excess B precursor and reaction byproducts are then purged from the chamber with nitrogen and precursor A is introduced again. The two half reactions are shown below [9,10]:

$$Al\text{–}OH^* + Al(CH_3)_3 \rightarrow Al\text{–}O\text{–}Al(CH_3)_2{}^* + CH_4 \quad (A)$$

$$Al\text{–}CH_3{}^* + H_2O \rightarrow Al\text{–}OH^* + CH_4 \quad (B)$$

The asterisks designate the surface species. The A and B precursors are trimethyl aluminum (TMA, $Al(CH_3)_3$) and water (H_2O), respectively. The process continues in this ABAB fashion, depositing one atomic layer at a time until the film is of the desired thickness.

3. Fabrication process

The ALD Al_2O_3-based resonators are formed by a bi-layer structure of ALD Al_2O_3 and e-beam evaporated Cr. The Cr is necessary as a conducting layer for electrostatic actuation since Al_2O_3 is a dielectric material. The Cr also serves as a reflective layer in the optical measurements described later in this paper. A schematic representation of the ALD resonator is shown in Fig. 2.

The fabrication process starts with a silicon wafer coated with an ALD Al_2O_3 layer (Fig. 3(a)). The temperature of the ALD Al_2O_3 deposition is 130 °C and 500 AB cycles are performed. The thickness of the resulting ALD Al_2O_3 is around 80 nm and can be measured by either profilometer or X-ray reflectivity (XRR). A 5-nm-thick Cr layer is then deposited on top of the ALD Al_2O_3 layer by electron beam evaporation (Fig. 3 (b)). Photoresist (PR) AZP 4210 is applied by spin-coating as a mask for subsequent Cr and ALD Al_2O_3 patterning (Fig. 3(c)). After UV exposure, the AZP 4210 is developed (AZ 400K:DI Water = 1:3) for 90 s (Fig. 3(d)). The Cr and ALD Al_2O_3 layers are patterned consecutively by CR-7 and 5% HF solution, respectively (Fig. 3(e) and (f)). The PR mask is then removed in acetone (Fig. 3(g)). Isotropic SF_6 plasma etching is performed at 75 W RF power with a 15.39 sccm flow rate to release the micro-scale structures (Fig. 3(h)). In order to reduce the local heating problem, etching is done for 1 min followed by 1 min of cooling, then etched for another minute, and so forth. The total etching time is 20 min. The fabrication results of the ALD micro resonators are shown in Fig. 4. The micro-resonators are completely released and the air gap is around 10 μm.

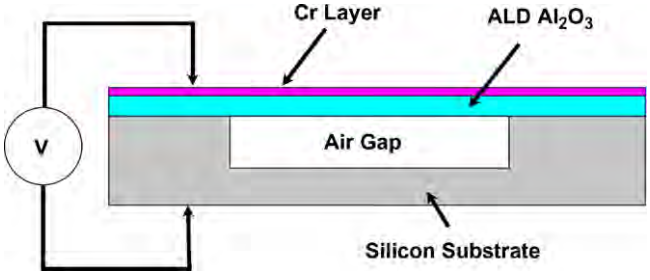

Fig. 2. Schematic representation of ALD resonator.

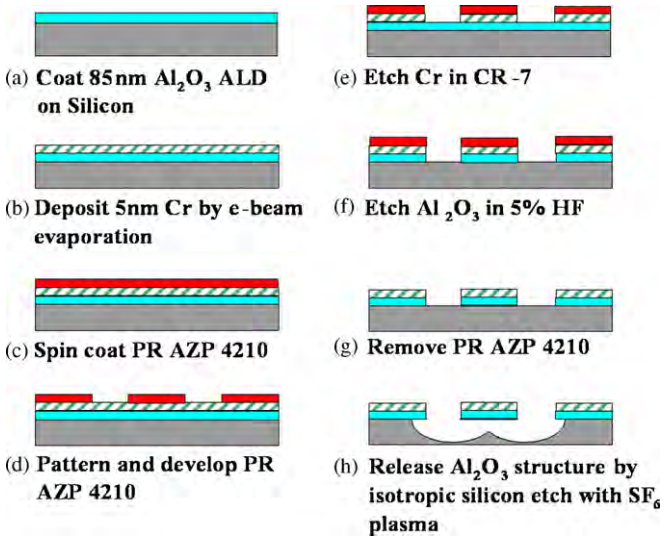

Fig. 3. Fabrication process of ALD-based resonator.

4. Displacement measurement

A technique to measure the profile of the ALD micro-resonators by an optical interferometer is described in this section. From the measured results, two models for clamped–clamped beams and pinned–pinned beams are compared with the experimental data. The measurement of displacement provides an estimation of the residue stress inside the structure. The resonant frequencies are then obtained from the resonance measurements in the following sections.

The 550-μm-long ALD Al_2O_3 micro-resonators are electrostatically actuated by the application of a DC voltage to the Cr pad and the silicon substrate. The range of DC voltage is from 0 V to 28 V. Zygo (NewView 200) [11], a white light interferometer, is used to

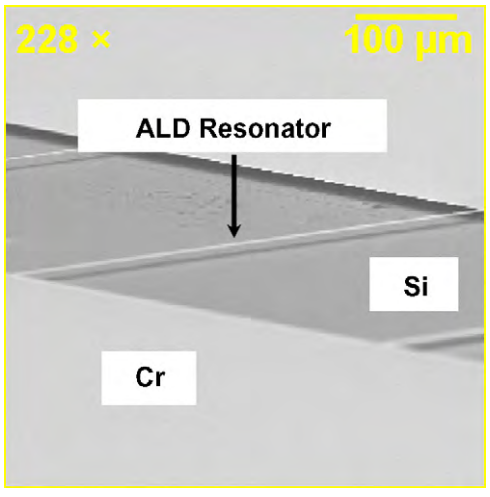

Fig. 4. SEM image of ALD Al_2O_3 micro-resonators.

Table 1
Parameters in the calculation of deflection.

Length of micro-resonator	550 μm
Width of micro-resonator	15 μm
Thickness of micro-resonator	0.085 μm
Young's modulus of ALD Al_2O_3	169 GPa
Dielectric constant of ALD Al_2O_3	6.8
Initial air gap	10 μm
Residual stress	250 MPa

measure the deflection of a micro-resonator.

A theoretical calculation of the displacement versus applied voltage is performed. The Young's modulus of ALD Al_2O_3 and Cr are 169 GPa [5] and 140 GPa [12], respectively. The structure is assumed to consist only of the ALD Al_2O_3 layer in the calculation, as the Cr layer is thin enough that its contribution can be neglected to the stiffness and thus effective spring constant of the structure. Moreover, residual stress in the structure dominates the spring constant and the error can thus be ignored. Consequently, the assumption of single Al_2O_3 layer is reasonable and simplifies the calculation.

First, the lumped model of a clamped–clamped micro-bridge with an axial residual stress and a uniform distributed transverse load is investigated. The length, width, and thickness of the micro-bridge are defined as L, W, and H, respectively in the analytical model. The Young's modulus of the structure is E. The spring constant, with residual stress, σ_0, can be expressed as [13]:

$$k_{stress-c} = \frac{4N}{\frac{L}{2} - 2\frac{\cosh(k_0 L/2)-1}{k_0 \sinh(k_0 L/2)}} \quad (1)$$

where $N = \sigma_0 WH$ represents the axial load caused by residual stress in the structure, and

$$k_0 = \sqrt{\frac{12N}{EWH^3}} \quad (2)$$

The units of the spring constant are N/m.

For a pinned–pinned micro-bridge with an axial residual stress and uniformly distributed transverse load (F_e), the spring constant can be expressed as

$$k_{stress-p} = \frac{\pi^5 EI + \pi^3 NL^2}{4L^3} \quad (3)$$

where

$$I = \frac{WH^3}{12} \quad (4)$$

The uniformly distributed transverse electrostatic force is expressed as [13]

$$F_e = \frac{1}{2}V^2 \left[\frac{\varepsilon_0 \varepsilon_{alumina} A}{(H + (Z_0 - z)\varepsilon_{alumina})^2}\right] \quad (5)$$

where V is the applied voltage, ε_0 is the permittivity of vacuum, $\varepsilon_{alumina}$ is the dielectric constant of ALD alumina, A is the micro-resonator area equal to $L \times W$, Z_0 is the initial gap, and z is the displacement at the center of micro-resonator.

The parameters used in the calculation are shown in Table 1. The thickness of ALD Al_2O_3 is measured by a profilometer and is 85-nm thick in this case. The measured profiles of the resonator with different applied voltages are compared with the theoretical calculation in Fig. 5. The profile of a pinned–pinned beam is assumed to be a simple sinusoidal function, which is expressed as

$$y(x) = y_0 \sin\frac{\pi x}{L} \quad (6)$$

where $y(x)$ is the displacement as a function of position, x, along the length. y_0 is the displacement at the central point of the structure,

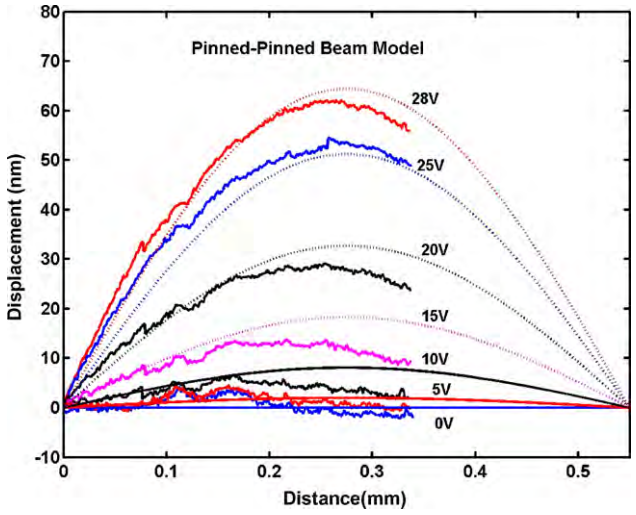

Fig. 5. Measured and theoretical calculated profiles of ALD Al_2O_3 micro-resonator with different applied voltages with 250 MPa residual stress.

i.e. at $x = L/2$, and is calculated based on the lumped model and Eq. (3).

The measured displacements at the central point of the resonator with different applied voltages are compared to the theoretical calculations with both clamped–clamped and pinned–pinned boundary conditions, and the results are shown in Fig. 6. With the residual stress of 250 MPa, both theoretical models fit to the experimental data. However, from the resonant frequency measurements in the next section, the results will reveal a better fit to the model with the pinned–pinned boundary condition. It is due to the small ratio of the thickness of the micro-resonator to its length, i.e. H/L, at only 0.01%. The resonator acts like a string instead like a bridge.

5. Resonant frequency measurement by SEM

A technique described in [15] is performed for the measurement of resonant frequencies as well as the Q factors of the ALD micro-resonators. This technique utilizes a scanning electron microscope (SEM) to detect the resonant frequency of ALD micro-resonators under a mechanical excitation by a piezoelectric stack. Meanwhile,

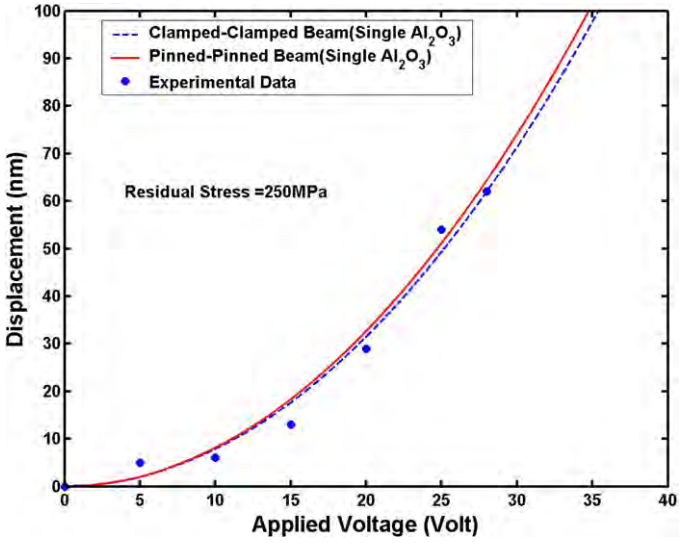

Fig. 6. Theoretical and experimental results of displacement vs. voltage of ALD Al_2O_3 micro-resonator with 250 MPa residual stress.

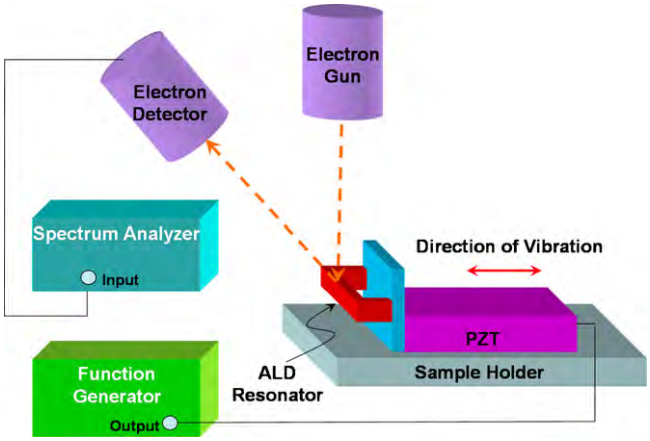

Fig. 7. Experimental setup with spectrum analyzer.

air-damping effect is eliminated in the measurement due to the high-vacuum environment in SEM. Two experimental setups are introduced in this paper. One setup with a spectrum analyzer provides a fast, broad-span detection of the different resonant modes while the other setup with a lock-in amplifier confirms the resonance by providing both its amplitude and phase information and provides a better Q value measurement with a higher scanning frequency resolution.

Another batch of devices was fabricated for resonant frequency measurements. The fabrication process is the same as described above. The dimensions of the ALD Al_2O_3 micro-resonators are the same as above, except the thickness. ALD Al_2O_3 thickness is 81 nm. The layer thicknesses are measured by *ex situ* (XRR).

For a pinned–pinned micro-bridge, the resonant frequency can be expressed as [14]

$$f_n = f_0\sqrt{1+\frac{\sigma_0 WHL^2}{\pi^2 EI}\left(\frac{1}{n}\right)^2}, \quad n = 1, 2, 3, \cdots \tag{7}$$

where

$$f_0 = \frac{(n\pi)^2}{2\pi L^2}\sqrt{\frac{EI}{\mu}} \tag{8}$$

In Eq. (8), μ is the mass per length and f_0 is the resonant frequency without the existence of residual stress.

The ALD alumina micro-resonators are placed in a SEM (JSM 6400 Scanning Microscope, JOEL, U.S.A. [11]) on a sample mount that carries a piezoelectric stack (AE0505D16, Thorlabs Inc., U.S.A. [11]). The resonance of the micro-resonator is driven by applying an AC signal to the piezoelectric stack at or near the resonant frequency. The direction of mechanical vibration of the piezoelectric stack is perpendicular to the substrate of the micro-resonator. The vibration of the ALD micro-resonator is detected via the secondary electron detector (scintillator followed by a photomultiplier tube (PMT)). By focusing the electron beam to a spot at the edge of the resonator, a different number of secondary electrons is produced depending on whether the resonator is in the path of the beam or not. The measurement is performed in a high vacuum chamber with pressure less than 10^{-6} Torr at room temperature.

Two different configurations of experimental setup are utilized for the higher mode observation and quality factor measurement, respectively. For the observation of higher modes, the PMT signal is fed into a real-time spectrum analyzer (RSA 3303A, Tektronix, U.S.A. [11]) and a white noise signal is generated by a function generator (DS345, Stanford Research Systems, U.S.A. [11]) to actuate the piezoelectric stack, as shown in Fig. 7. The amplitudes of the noise signal are 0.5 Vpp, 1 Vpp, and 2 Vpp, respectively, for observing different modes. Stronger signal is needed for the observation of higher modes. With the real-time spectrum analyzer, a broad scanning frequency range within a short time is allowed at the cost of losing phase sensitivity.

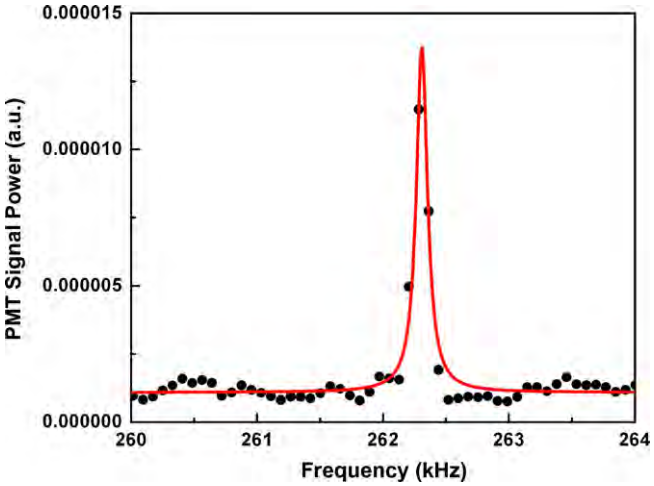

Fig. 8. First mode of ALD alumina resonator (8 μm wide, 550 μm long and 81 nm thick).

A micro-resonator is measured. The dimension of the resonator is 550 μm in length, 8 μm in width, and 81 nm in thickness. The first six modes are measured and shown in from Figs. 8–13. The experimental data are fit to the magnitude of a standard Lorentzian function, which is expressed as

$$H(w) = \frac{A}{w^2 - w_n^2 - iw\Gamma} \tag{9}$$

In Eq. (9), A is a constant, w_n is the resonant frequency of nth mode in rad/s, w is the driving frequency, and Γ is damping coefficient.

The resonant frequencies and quality factors are extracted from the Lorentzian model after the curve fittings and are listed in Table 2. The quality factors are determined by the ratio of resonant frequency to the width of the resonance peak (Full Width Half Maximum), which is expressed as

$$Q = \frac{f_n}{\Delta f_{\mathrm{FWHM}}} \tag{10}$$

The experimental data and calculated frequencies by both pinned–pinned and clamped–clamped beam model are compared

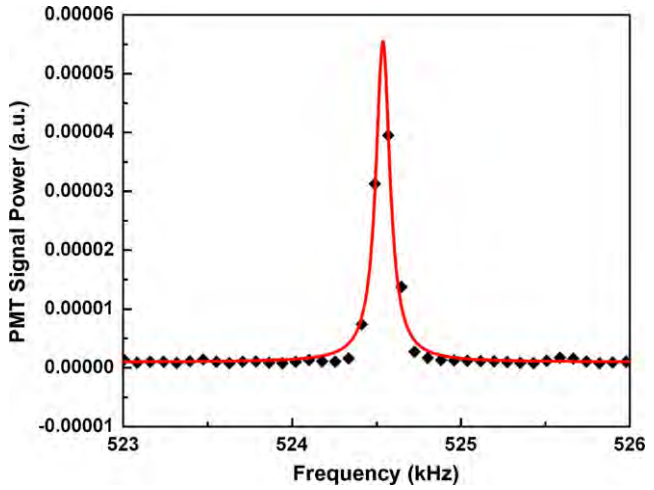

Fig. 9. Second mode of ALD alumina resonator (8 μm wide, 550 μm long and 81 nm thick).

Table 2
Measured and calculated resonant frequencies and measured quality factors of the first six modes of an ALD alumina resonator (8 μm wide, 550 μm long and 81 nm thick).

Mode	Resonant frequency (Hz)	Calculated frequency (Hz)	FWHM (Hz)	Quality factor	Amplitude of drive signal (V)
1	262,308	262,688	107	2,451	0.5
2	524,538	525,388	101	5,193	0.5
3	787,542	788,108	244	3,228	0.5
4	1,050,368	1,050,861	61	17,219	1
5	1,312,750	1,313,657	486	2,701	1
6	1,575,502	1,576,506	526	2,995	2

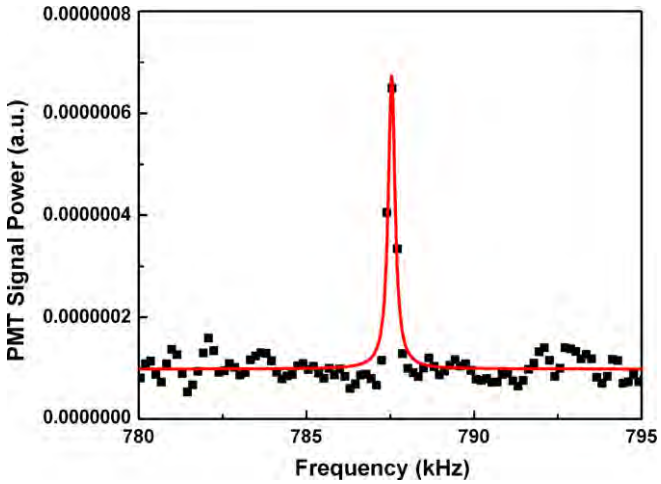

Fig. 10. Third mode of ALD alumina resonator (8 μm wide, 550 μm long and 81 nm thick).

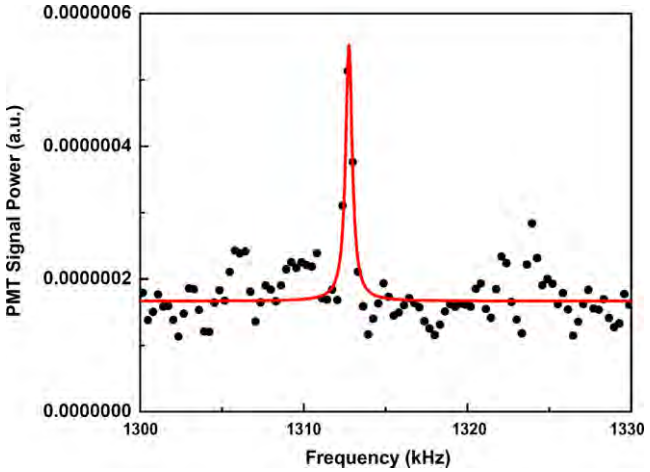

Fig. 12. Fifth mode of ALD alumina resonator (8 μm wide, 550 μm long and 81 nm thick).

as shown in Fig. 14. By inserting the residual stress of 258 MPa, the calculated resonant frequencies of the first six modes with the pinned–pinned beam model match the measured frequencies better than the clamped–clamped beam model. The calculated resonant frequencies with pinned-pinned beam model are listed in Table 2. The differences between the measured and calculated frequencies are within 1 kHz.

In the second setup (Fig. 15), PMT signal is fed into the input channel of a lock-in amplifier (SR844, Stanford Research Systems, U.S.A. [11]) while a synchronized signal from the function generator is fed into the reference channel. The configuration with a lock-in amplifier allows a phase sensitive analysis with slow sweeping of frequency. Meanwhile, an attenuator with 28 dB attenuation is added to the coaxial cable to the piezoelectric stack in order to reduce the vibration amplitude while the amplitude of sinusoidal wave from the function generator is 0.01 Vpp.

A 4 μm wide micro-resonator with the same length and thickness as the one described above was then measured. The in-phase and out-of-phase PMT signal amplitudes versus applied signal frequency are recorded and shown in Fig. 16. By fitting with the Lorentzian model, the first resonant frequency and the width of resonance are extracted to be 265,698 Hz and 6 Hz, respectively. The measured Q factor is then calculated to be over 39,000 for the 4 μm bridge.

6. Resonant frequency measurement by AFM

Another technique is developed for the measurement of resonant frequency with AFM under electrical excitation, rather than

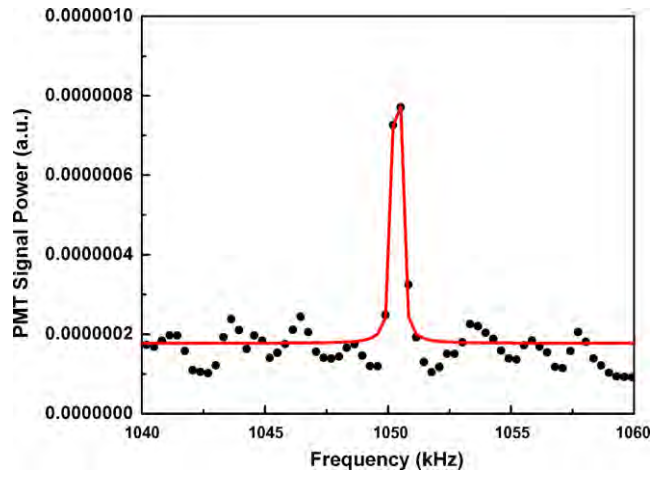

Fig. 11. Fourth mode of ALD alumina resonator (8 μm wide, 550 μm long and 81 nm thick).

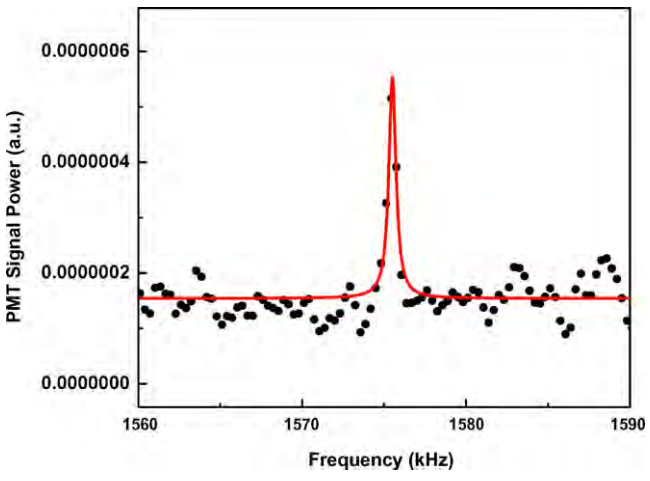

Fig. 13. Sixth mode of ALD alumina resonator (8 μm wide, 550 μm long and 81 nm thick).

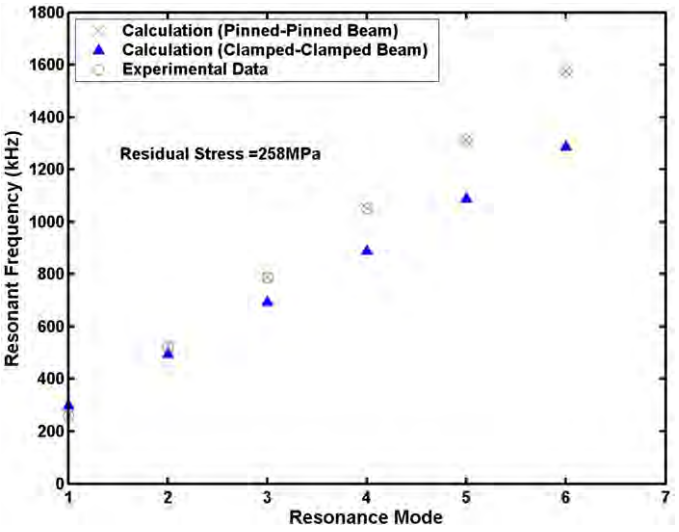

Fig. 14. Calculated resonant frequencies with 258 MPa residual stress match with the measured resonant frequencies (○) for ALD alumina resonator (8 μm wide, 550 μm long and 81 nm thick). The frequencies with the both models of pinned–pinned beam (×) and clamped–clamped beam (▲) are calculated with 258 MPa residual stress.

the mechanical excitation in the SEM technique (Fig. 7). This technique is important as it is a complementary way to the SEM and optical techniques of measuring the resonant frequencies of the ALD bridges. This technique has already been used to measure the resonance response of a dense mat of DNA [17] and carbon nanotubes [19]. We applied this technique to measuring vibration modes of ALD bridges in this paper. First we discuss the experimental technique and then we will show two measured modes and discuss the theory behind the measurement.

The experiment is carried out using a modified, commercially available atomic force microscope (AFM) as shown in Fig. 17. The Si AFM cantilever sits on a XYZ piezo-stage for scanning across the sample. The distance between the cantilever and the sample is held fixed via an AC-mode feedback loop [16], with dither frequency, f_1, of 15.0 kHz being the fundamental mode of the 500 μm long Si cantilever. The sample stage is a home-made Al stage which has a UT-085 coaxial cable and connector integrated into it to bring the signal from a variable frequency source. The source frequency can be varied from 100 kHz to 1.05 GHz, and is amplified about 25 dB. The system with the present SMA connector is capable of frequency measurements up to 18 GHz. The source frequency is modulated at frequency f_2 of 92.3 kHz, which is the second resonance mode

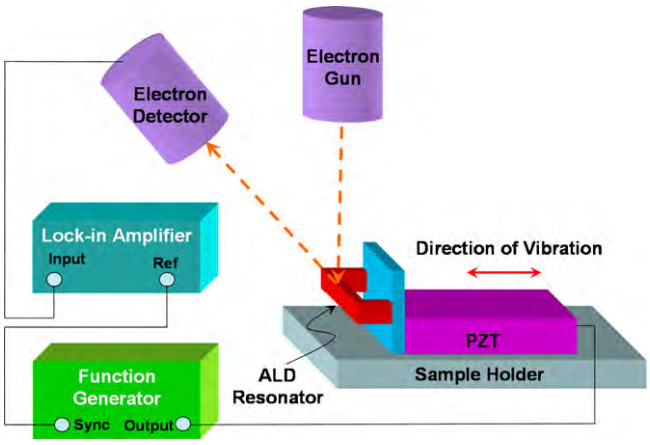

Fig. 15. Experimental setup with lock-in amplifier.

of the cantilever, using an approach similar to multi-frequency amplitude-modulated AFM [17]. The vibration of the ALD micro-bridge is measured with a lock-in detection scheme. The whole set-up sits in an ambient environment on a vibration isolation stage with resonance frequency of 2 Hz. The whole AFM and vibration isolation assembly is placed in a box to isolate it from air currents in the room.

An AC-mode topographic image of the bridge is acquired in order to align the tip of the cantilever with the center of the ALD micro-bridge. The cantilever is then positioned over the center of the ALD micro-bridge, while the AFM feedback circuit maintains a constant separation between the cantilever and the micro-bridge. At this time the variable frequency source, lock-in amplifier and modulation frequency are turned on. This excites the vibration of the ALD bridge in response to the time-varying, capacitive coupled electromagnetic signal. Knowing before hand the calculated resonance frequencies of the given ALD micro-bridge, we pick a narrow bandwidth of few kHz around the expected resonance, and then sweep the frequency around the resonance. When the source excites a mechanical vibration mode in the ALD micro-bridge, then the amplitude of the cantilever deflection at f_2 increases. This deflection signal is detected using a lock-in detection technique at f_2 of 92.3 kHz.

The experiments were performed in ambient environment, in contrast to the SEM technique shown in Fig. 7 where the measurements are performed in vacuum. As a result we expect the measured resonant frequencies to be shifted slightly and the measured Q of the bridges to be significantly lower. For a 15-μm wide pinned–pinned ALD bridge with the same length and thickness described above, the first four calculated modes are 262.7 kHz, 525.4 kHz, 788.1 kHz and 1050.9 kHz with residual stress of 258 MPa. For this particular bridge, the deflection signal is detected using a lock-in detection technique at f_2 of 92.3 kHz. The results of the measurement are shown in Fig. 18, and the data has been smoothed using a binomial smoothing filter. We show the first and the fourth mode of the 15 μm bridge in Fig. 18. The lock-in detection technique is important here, as we detect a very weak signal from the bridge. The signal is weak, as the amplitude of mechanical vibration is small, and the source signal to excite the bridges weakens significantly as it passes through 500 μm of silicon substrate supporting the sample (Fig. 17). We measure the resonant frequency for mode 1 at 270.6 kHz and mode 2 at 411.8 kHz (not shown).

The reason we measure at half the resonant frequency of the mode (see Figs. 8–13) is due to the V^2 dependence in the force

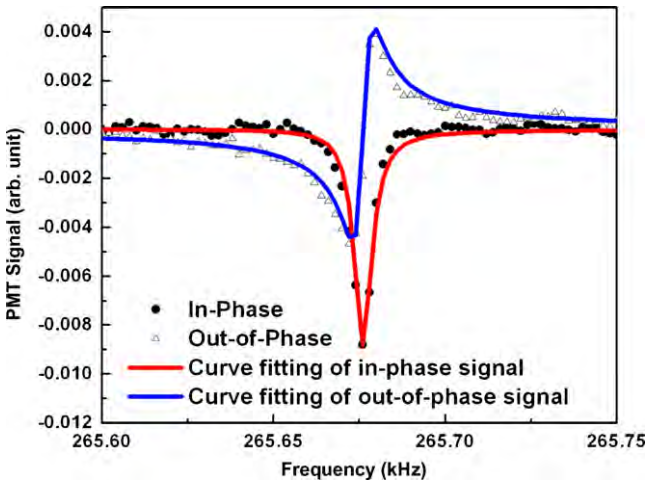

Fig. 16. Measured in-phase and out-of phase signals of the 1st resonant mode of ALD alumina micro-resonator (4 μm wide, 550 μm long, and 81 nm thick).

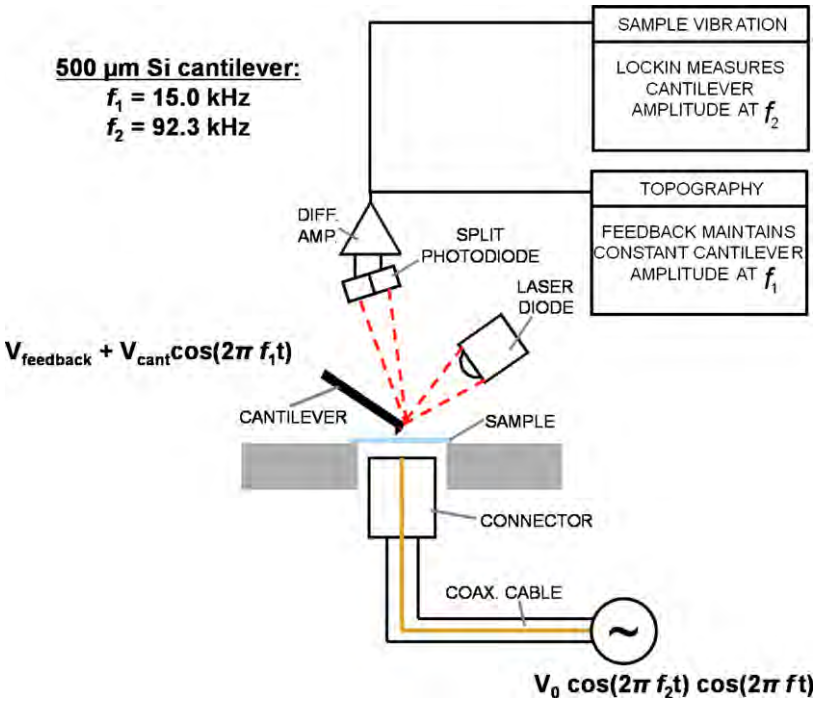

Fig. 17. Experimental setup of AFM used for measurement of ALD micro-bridge resonances. The dither frequency for the AC mode AFM is f_1 to measure the topography of the bridge. The low-frequency signal from the source at frequency f is used to excite the mechanical resonance modes in the bridge. The frequency f is modulated at f_2 and lock-in detection scheme is used to measure the excited mechanical modes.

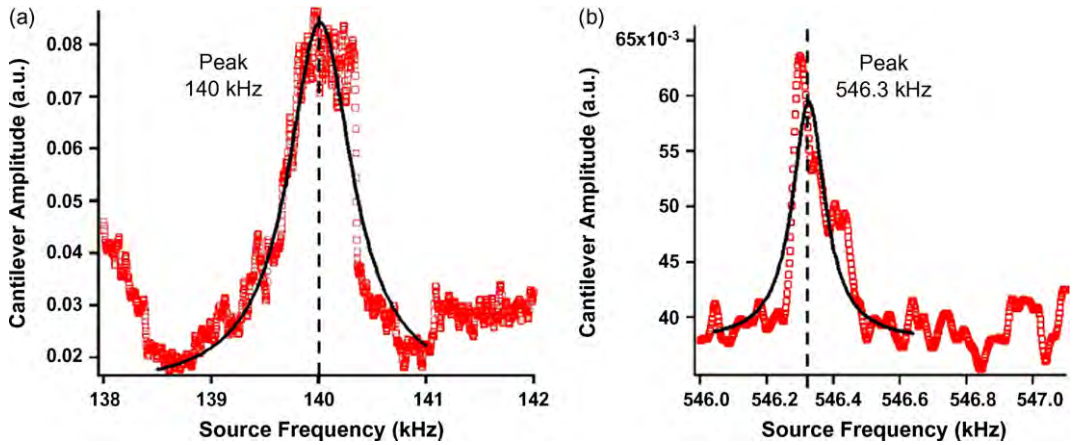

Fig. 18. The cantilever amplitude at 92.3 kHz. (a) According to the theory, the first mode of the ALD bridge is at 262.7 kHz and (b) the fourth mode is at 1050.9 kHz. The resonant frequency of the bridge is twice the driving frequency which is shown in the graphs. This is due to the non-linear dependence of force on the driving signal from the source as explained in the text. The data shown is average of eight frequency sweep and the measurement took about 8 h each. The fits are just for the guidance to the eye.

term [18] similar to Eq. (5). The ALD micro-bridge and the silicon substrate form two electrodes of the parallel plate capacitor with capacitance:

$$C = \varepsilon_0 \frac{A}{d} \tag{11}$$

and stored energy U,

$$U = \frac{1}{2} CV^2 \tag{12}$$

where A is the area of the capacitor, d is the separation between the electrodes and V is the voltage across the capacitor. In the limit of small amplitude change, the separation changes by amount δd, making the net capacitance change to be

$$\delta C = -\frac{\varepsilon_0 A \delta d}{d^2} \tag{13}$$

The change in energy (which is proportional to the force F [18]), is

$$\delta U = \frac{1}{2}\delta C V^2 + CV\delta V = \frac{1}{2}\delta C V_0^2 \cos^2(2\pi f_2 t)\left[\frac{1}{2} + \frac{1}{2}\cos(2\pi(2f)t)\right] + CV_0\delta V \cos^2(2\pi f_2 t)\left[\frac{1}{2} + \frac{1}{2}\cos(2\pi(2f)t)\right] \tag{14}$$

measured by the deflection amplitude of the cantilever with $V = V_0 \cos(2\pi f_2 t)\cos(2\pi f t)$. This means that the resonant frequency of the micro-bridge is twice the driving frequency used to excite the ALD micro-bridge.

7. Conclusions

In summary, micromachined ALD Al_2O_3 resonators are demonstrated in this paper. Due to the high quality of ALD produced

materials, there is great promise for nano-scale resonators based on this technology in future applications. The results and methods presented in this paper are applicable for future design of nanometer-scale ALD-based devices. The profiles of fabricated ALD resonators are measured at different applied voltages using optical interferometer to estimate the residual stress in the structure. The resonant frequencies are measured for several resonators. An axial thin film stress in the resonators of 258 MPa is determined by best fitting to the experimental data. Two different techniques for measurement of resonant frequency are developed. The first method, the experimental setup utilizing SEM provides a mechanical excitation method to measure the resonant frequency of micro-/nano-electromechanical resonators. Higher modes may be easily measured by the experimental setup with spectrum analyzer while higher Q factor may be measured by the experimental setup with lock-in amplifier. With this method, however, the resonant frequency measurement is limited to around 3 MHz due to the bandwidth in the secondary electron detector. The second method, the experimental setup utilizing AFM provides the solution for high resonant frequency measurement for nano-scale electromechanical resonators up to GHz range. A similar method has been demonstrated for GHz range frequency measurement of carbon nanotubes [19]. The measurement, however, is conducted in atmospheric pressure at room temperature. The measured Q factor is thus substantially decreased.

Acknowledgements

The DARPA/MTO and SPAWAR Grant No: N66001-07-1-2033 is gratefully acknowledged for the financial support. The authors would like to thank Wendy Krauser and Muhong Lin in the Department of Mechanical Engineering at CU-Boulder for the lithography masks. Yuan-Jen Chang would also like to thank Dr. Martin Dunn in the Department of Mechanical Engineering for valuable discussions about the modeling and Keith Cobry in the Department of Mechanical Engineering for SF_6 etching.

References

[1] G. Stemme, Resonant silicon sensors, J. Micromech. Microeng. 1 (1991) 113–125.
[2] A.N. Cleland, M. Pophristic, I. Ferguson, Single-crystal aluminum nitride nanomechanical resonators, Appl. Phys. Lett. 79 (2001) 2070–2072.
[3] N.D. Hoivik, J.W. Elam, R.J. Linderman, V.M. Bright, S.M. George, Y.C. Lee, Atomic layer deposited protective coatings for micro-electromechanical systems, Sens. Actuators A 103 (2003) 100–108.
[4] M.K. Tripp, C. Stampfer, D.C. Miller, T. Helbling, C.F. Herrmann, C. Hierold, K. Gall, S.M. George, V.M. Bright, The mechanical properties of atomic layer deposited alumina for use in micro- and nano-electromechanical systems, Sens. Actuators A 130–131 (2006) 419–429.
[5] M.K. Tripp, C.F. Herrmann, S.M. George, V.M. Bright, Ultra-thin multilayer nanomembranes for short wavelength deformable optics, in: Tech. Digest IEEE International Conference on Micro Electro Mechanical Systems (MEMS'04), Maastricht, The Netherlands, January 25–29, 2004, pp. 77–80.
[6] D.S. Finch, T. Oreskovic, K. Ramadurai, C.F. Herrmann, S.M. George, R.L. Mahajan, Biocompatibility of atomic layer-deposited alumina thin films, J. Biomed. Mater. Res. A 87 (1) (2007) 100–106.
[7] Y.J. Chang, K. Cobry, V.M. Bright, Atomic layer deposited alumina for micromachined resonators, in: Tech. Digest IEEE International Conference on Micro Electro Mechanical Systems (MEMS'08), Tucson, AZ, U.S.A., January 12–17, 2008, pp. 387–390.
[8] S.M. George, A.W. Ott, J.W. Klaus, Surface chemistry for atomic layer growth, J. Phys. Chem. 100 (31) (1996) 13121–13131.
[9] A.C. Dillon, A.W. Ott, J.D. Way, S.M. George, Surface chemistry of Al_2O_3 deposition using $Al(CH_3)_3$ and H_2O in a binary reaction sequence, Surf. Sci. 322 (1–3) (1995) 230–242.
[10] A.W. Ott, J.W. Klaus, J.M. Johnson, S.M. George, Al_3O_3 thin film growth on Si(1 0 0) using binary reaction sequence chemistry, Thin Solid Films 292 (1–2) (1997) 135–144.
[11] Use of trade names does not imply the endorsement by U.S. Government.
[12] B. Hälg, On a nonvolatile memory cell based on micro-electro-mechanics, in: Tech. Digest IEEE International Conference on Micro Electro Mechanical Systems (MEMS'90), Napa Valley, California, February 11–14, 1990, pp. 172–176.
[13] S.D. Senturia, Microsystem Design, Kluwer Academic Publishers, Massachusetts, USA, 2001.
[14] R.D. Blevins, Formulas for Natural Frequency and Mode Shape, Van Nostrand Reinhold Co., New York, USA, 1979.
[15] S.M. Tanner, J.M. Gray, C.T. Rogers, High-Q GaN nanowire resonators and oscillators, Appl. Phys. Lett. 91 (2007) 203117.
[16] C.J. Chen, Introduction to Scanning Tunneling Microscopy, 2nd edition, Oxford University Press, 2008 (Chapter 15).
[17] R. Proksch, Multifrequency, repulsive-mode amplitude-modulated atomic force microscopy, Appl. Phys. Lett. 89 (2006) 113121.
[18] Y. Seo, W. Jhe, Atomic force microscopy and spectroscopy, Rep. Prog. Phys. 71 (2008) 016101.
[19] D. Garcia-Sanchez, A. San Paulo, M.J. Esplandiu, F. Perez-Murano, L. Forro, A. Aguasca, A. Bachtold, Mechanical detection of carbon nanotube resonator vibrations, Phys. Rev. Lett. 99 (2007) 085501.

Biographies

Yuan-Jen Chang earned a BS in mechanical engineering at National Taiwan University, Taiwan, in 1996 and a MS in the department of aeronautics and astronautics at National Cheng Kung University, Taiwan, in 1998. He has worked at the Industrial Technology Research Institute (ITRI), Taiwan, as a mechanical design engineer from 2000 to 2002. He is currently a PhD student in mechanical engineering at the University of Colorado at Boulder. His current research interests include applications of electrowetting on dielectric, optical MEMS, micro- and nano-fabrication techniques, and the applications of ALD thin films.

Jason M. Gray earned a BA in physics with a minor in mathematics from the University of Colorado at Boulder in 2004. He is currently a PhD student in physics at the same university. His research involves measuring electrical and mechanical properties of GaN nanowires grown at the National Institute of Standards and Technology (NIST) in Boulder.

Atif Imtiaz is currently a National Research Council (NRC) Post-Doctoral Fellow in the Electromagnetics Division at the National Institute of Standards and Technology (NIST) at Boulder, Colorado. He received his PhD in Physics from University of Maryland at College Park in 2005. He has received his BS in Physics from State University of New York at Stony Brook in 1998. His overall research interest has been in fundamental and applied aspects of solid-state physics. He has been active in near-field radio and microwave measurements which include developing radio-frequency scanning tunneling (rf-STM) microscope and radio-frequency atomic force microscope (rf-AFM).

Dragos Seghete received his BS degree with honors (magna cum laude) in Chemistry and Mathematics from University of Arkansas, Fayetteville, AR in 2005. He is currently a physical chemistry PhD student at the University of Colorado at Boulder. His research interests include the exploration of new chemistries for the atomic layer deposition of low-density films and the development of new applications for existing ALD systems.

T. Mitch Wallis received his BS degree in physics from the Georgia Institute of Technology in 1996 and his MS and PhD degrees in physics from Cornell University in 2000 and 2003, respectively. In 2003, he was awarded a National Research Council postdoctoral fellowship at the National Institute of Standards and Technology. From 2005 to 2007, he held a postdoctoral appointment at Colorado State University. Presently, he is a physicist at NIST. His research interests include the development of high-frequency scanning probe microscopes and other metrology for high-speed nanoscale electronics and spintronics.

Steven M. George is professor in the Department of Chemistry and Biochemistry and Department of Chemical and Biological Engineering at the University of Colorado at Boulder. Dr. George received his BS in Chemistry from Yale University (1977) and his PhD in Chemistry from the University of California at Berkeley (1983). He has more than 200 peer-reviewed publications in the areas of thin film growth, surface science and physical chemistry. Dr. George is a Fellow of the American Vacuum Society (2000) and a Fellow of the American Physical Society (1997). Dr. George's research interests are in the areas of surface chemistry, thin film growth and nanostructure engineering. He is currently directing an internationally recognized research effort focusing on atomic layer deposition (ALD) and molecular layer deposition (MLD). This research is examining new surface chemistries for ALD and MLD growth, measuring thin film growth rates, characterizing the properties of thin films and developing new reactors for film growth. Dr. George served as Chair of the first American Vacuum Society (AVS) Topical Conference on Atomic Layer Deposition (ALD2001) held in Monterey, California. He also teaches a one-day short course on ALD for the AVS. In addition, Dr. George is a co-founder of ALD NanoSolutions, Inc., a startup company that is working to commercialize ALD technology.

Pavel Kabos received his MS degree with first class honors in Solid State Physics from Slovak University of Technology in 1970 and PhD and habilitation (DSc) degrees from the same University in 1979 and 1994, respectively. Since 1972 he was associated with the Department of Electromagnetic Theory at the Faculty of Electrical Engineering and Information Technology as an assistant, and since 1983 as an associate professor. During years 1982/1984 he worked as a postdoctoral fellow at the department of Physics, Colorado State University, where he returned in 1991 and worked

as a visiting scientist, and later as a research professor, addressing the problems of linear and nonlinear high frequency magnetism. In the 1980s and 1990s he was a postdoctoral fellow, visiting scientist, and research professor at Colorado State University. In 1998 he joined the National Institute of Standards and Technology, Boulder, as a visiting scientist and became a staff physicist in the Electromagnetics Division in 2001. Dr. Kabos research is on linear and nonlinear precession dynamics, metrology for high-speed electronics, magnetic force microscopy, dielectric and magnetic materials spectroscopy, non-destructive electromagnetic evaluation, and numerical methods for electromagnetic field analysis. He has authored or co-authored over 100 archival papers on magnetics, several book chapters, and one book, *Magnetostatic Waves and Their Applications*. He is IEEE fellow.

Charles T. Rogers works on small devices fabricated with electron-beam lithography, on phase transitions and dynamical processes in reduced dimensional systems, and on the physics of fluctuations and noise in very small electronic devices. Prof. Rogers received his PhD degree in Applied Physics from Cornell University in 1987. He spent 6 years working as a Member of Technical Staff in Solid State Physics at Bellcore. He has been at the University of Colorado, Department of Physics since 1992 (professor of Physics since 2003). He has recently served as director of the Engineering Physics Program at the University of Colorado (2001–2004), interim chair for the Department of Physics (May–August 2005), as associate chair for Undergraduate Programs in the Department of Physics (2003–2006). He has published over 90 peer reviewed papers, has two patents, and has advised the research projects for 14 graduate students and 6 post-doctoral scientists.

Victor M. Bright received his BSEE degree from the University of Colorado at Denver in 1986, and the MS and PhD degrees from the Georgia Institute of Technology, in 1989 and 1992, respectively. Dr. Bright is currently the Alvah and Harriet Hovlid Professor of Mechanical Engineering and the faculty director for Discovery Learning, College of Engineering and Applied Science (CEAS), University of Colorado at Boulder. From 2005 through 2007, he served as the associate dean for Research, CEAS, CU-Boulder. Prior to joining the University of Colorado, he was a professor in the Department of Electrical and Computer Engineering, Air Force Institute of Technology, Wright-Patterson Air Force Base, Ohio (1992–1997). During 2004 he was a visiting professor at the Swiss Federal Institute of Technology (ETH-Zurich), Switzerland. Prof. Bright's research activities include micro- and nano-electromechanical systems (MEMS and NEMS), silicon micromachining, microsensors/microactuators, opto-electronics, optical, magnetic and RF microsystems, atomic-layer deposited materials, ceramic MEMS, MEMS reliability, and MEMS packaging. Dr. Bright has served on the Executive Committee of the ASME MEMS Division, on the Technical Program Committee of the IEEE MEMS 2000 through 2006 conferences, and as the General Co-Chair for the IEEE MEMS 2005 International Conference. He also served on the Technical Program Committee for the Transducers'03, Transducers'07 and IEEE/LEOS Optical MEMS 2003 through 2005. He has taught a Short Course on MEMS Packaging at Transducers'03 and Transducers'05. Prof. Bright is a senior member of IEEE, a fellow of ASME, and an author of over 250 journal papers, conference proceedings, and book chapters in the fields of MEMS, NEMS and microsystems.